

Free Vibration Solution for Clamped Orthotropic Plates Using Lagrangian Multiplier Technique

R. L. Ramkumar,* P. C. Chen,† and W. J. Sanders‡

Northrop Corporation, Hawthorne, California

Using the Lagrangian multiplier technique, an analysis was developed to compute the natural frequencies and mode shapes of clamped orthotropic laminated plates. Transverse shear deformation effects were included using a higher-order plate theory. Predictions made with the developed analysis demonstrated excellent agreement with the available experimental test results and other analytical solutions. The validated free vibration analysis has also been used to develop an analysis to predict the dynamic response of clamped orthotropic plates subjected to low-velocity impact by a hard object.

Nomenclature

| | |
|----------|------------------------------|
| a | =length of the plate |
| A_{ij} | =inplane stiffness |
| b | =width of the plate |
| D_{ij} | =bending stiffness |
| g | =acceleration due to gravity |
| h | =thickness of the plate |
| γ | =laminar weight density |
| ω | =natural frequency |

Subscripts

x, y, z, t = derivatives of ()

Introduction

AN analytical prediction of the dynamic mechanical response of a plate involves the computation of its natural frequencies and mode shapes. This analysis can be performed easily and in closed form only when the plate is isotropic or specially orthotropic and is constrained by simple supports at the boundaries.^{1,2} The problem increases in complexity when the plate exhibits general anisotropy. In this case, even when the boundaries are simple supports, one must resort to approximate analytical procedures. If the boundaries are clamped, approximate solutions are the only possibility, even for isotropic plates. And, if the plate thickness is not negligible in comparison to planform dimensions, shear deformation effects have to be accounted for, necessitating a higher-order analysis.^{3,4}

Analysis

Figure 1 defines the geometry and reference coordinates for the analyzed laminated plate. The plate length, width, and thickness dimensions are a , b , and h , respectively, and its reference coordinates x , y , and z . The fiber coordinates for the individual plies in the laminate are 1, 2, and 3, as shown in Fig. 1. Transverse shear deformation effects are accounted for using a higher-order plate theory,^{3,4} assuming a Mindlin shear correction factor K of $\pi^2/12$. Linear strain-displacement relationships are used, assuming small displacement gra-

dients.^{1,2} Also, the laminate is assumed to be midplane symmetric and in-plane (membrane) displacements are assumed to be negligible compared to flexural displacements.

The total strain energy V in the laminate is expressed as

$$V = \frac{1}{2} \iint_{\text{Area}} \left[KA_{44}(w_{,y} + \psi_y)^2 + KA_{55}(w_{,x} + \psi_x)^2 + 2KA_{45}(w_{,x}w_{,y} + w_{,x}\psi_y + w_{,y}\psi_x + \psi_x\psi_y) + D_{11}\psi_{x,x}^2 + 2D_{12}\psi_{x,x}\psi_{y,y} + D_{22}\psi_{y,y}^2 + 2D_{16}\psi_{x,x}(\psi_{x,x} + \psi_{y,x}) + 2D_{26}\psi_{y,y}(\psi_{x,y} + \psi_{y,x}) + D_{66}(\psi_{x,y} + \psi_{y,x})^2 \right] \quad (1)$$

where A_{ij} and D_{ij} are the laminate in-plane and bending stiffnesses, respectively,^{1,2} w the plate displacement in the Z direction, ψ_x and ψ_y the midplane slopes in the xz and yz planes, respectively, and $w_{,x}$, $\psi_{x,x}$ the derivatives of w and ψ_x with respect to x , etc. D_{16} and D_{26} are zero for a specially orthotropic laminate.^{1,2}

Ignoring rotatory inertia effects and in-plane effects, the kinetic energy T of the laminated plate is expressed as

$$T = \frac{1}{2} m w_{,t}^2 = \frac{\gamma h}{2g} \int_0^a \int_0^b w_{,t}^2 dx dy \quad (2)$$

where γ is the laminate weight density, h the plate thickness, and g the acceleration due to gravity (see Fig. 1).

In the reported effort, the free vibration problem was solved using the Lagrangian multiplier technique.⁵⁻⁷ Solutions to similar eigenvalue problems have been obtained by other investigators using the Rayleigh-Ritz approach.⁸ The Lagrangian multiplier method, like the Rayleigh-Ritz method, uses energy principles to provide an approximate analytical solution when a closed-form solution cannot be obtained. The plate variables (w , ψ_x , and ψ_y) are assumed to be series expressions with undetermined coefficients. Boundary conditions not satisfied by the assumed series expressions are imposed as constraint conditions. The total energy expression for the plate (including the strain energy, the kinetic energy, and the energy corresponding to the imposed constraints) is subsequently minimized with respect to the undetermined coefficients in the assumed series. The constraint conditions and this minimization process yield a set of linear homogenous equations in terms of the undetermined coefficients and Lagrangian multipliers. The natural frequencies and mode shapes of the plate are obtained by solving the corresponding

Received Aug. 29, 1985; revision received April 16, 1986. Copyright © American Institute of Aeronautics and Astronautics, Inc., 1986. All rights reserved.

*Manager, Composite Manufacturing Technology, Aircraft Division.

†Engineering Specialist, Manufacturing Technology, Aircraft Division.

‡Senior Engineer, Dynamic Loads/Advanced Systems Division.

eigenvalue problem. A brief description of the Lagrangian multiplier technique is presented in the following.

Lagrangian Multiplier Method

Assume that a function $f(x_1, x_2, \dots, x_p)$ is to be minimized with respect to the p independent variables x_1, x_2, \dots, x_p , subject to the following q constraining relationships:

$$\phi_j(x_1, x_2, x_3, \dots, x_p) = 0, \quad j = 1, 2, 3, \dots, q \quad (3)$$

The Lagrangian multiplier method minimizes the following function with respect to the independent variables:

$$f(x_1, x_2, \dots, x_p) - \sum_{j=1}^q \lambda_j \phi_j(x_1, x_2, \dots, x_p) \quad (4)$$

where λ_j are unknown Lagrange multipliers. The minimization process yields the following p equations:

$$\frac{\partial f}{\partial x_i} - \lambda_1 \frac{\partial \phi_1}{\partial x_i} - \lambda_2 \frac{\partial \phi_2}{\partial x_i} - \dots - \lambda_q \frac{\partial \phi_q}{\partial x_i} = 0 \quad i = 1, 2, 3, \dots, p \quad (5)$$

These p minimization equations and q constraint equations provide the solutions for the $p \times q$ unknowns $(x_1, x_2, \dots, x_p, \lambda_1, \lambda_2, \dots, \lambda_q)$.

Eigenvalue Solutions for Clamped Orthotropic Laminates

The following boundary conditions apply to the clamped laminated plate in Fig. 1:

$$w(0, y, t) = w(a, y, t) = w(x, 0, t) = w(x, b, t) = 0 \quad (6)$$

$$\psi_x(0, y, t) = \psi_x(a, y, t) = \psi_y(x, 0, t) = \psi_y(x, b, t) = 0 \quad (7)$$

Series expressions for the transverse plate displacement and its midplane bending slopes are assumed to be

$$w(x, y, t) = \sum_m \sum_n a_{mn} \sin\left(\frac{m\pi x}{a}\right) \sin\left(\frac{n\pi y}{b}\right) Z(t) \quad (8)$$

$$\psi_x(x, y, t) = \sum_m \sum_n b_{mn} \cos\left(\frac{m\pi x}{a}\right) \sin\left(\frac{n\pi y}{b}\right) Z(t) \quad (9)$$

$$\psi_y(x, y, t) = \sum_m \sum_n d_{mn} \sin\left(\frac{m\pi x}{a}\right) \cos\left(\frac{n\pi y}{b}\right) Z(t) \quad (10)$$

where a_{mn} , b_{mn} , and d_{mn} are unknown coefficients and $Z(t)$ a function of time t . Equation (8) satisfies the boundary displacement conditions, but Eqs. (9) and (10) do not satisfy the boundary slope conditions. The following constraint conditions must be satisfied by the unknown coefficients in order to impose the unsatisfied zero-slope boundary conditions:

$$\sum_m b_{mj} = 0, \quad j = 1, 2, 3, \dots, q \quad (11)$$

$$\sum_n d_{in} = 0, \quad i = 1, 2, 3, \dots, p \quad (12)$$

The free vibration (natural) frequencies and the corresponding mode shapes for the clamped laminate are obtained

by assuming the time-dependent function in Eqs. (8-10) to be harmonic. Setting $Z(t)$ to be $\exp(i\omega t)$, the total strain energy in the plate [Eq. (1)] is expressed as

$$V = \left(\frac{ab\pi^2}{4}\right) \sum_m \sum_n [E_{mn} a_{mn}^2 + F_{mn} b_{mn}^2 + G_{mn} d_{mn}^2 + 2H_m a_{mn} b_{mn} + 2U_n a_{mn} d_{mn} + 2Q_{mn} b_{mn} d_{mn}] \exp(2i\omega t) \quad (13)$$

where E_{mn} , etc., are defined as

$$\begin{aligned} E_{mn} &= (K/2) [A_{44}(n/b)^2 + A_{55}(m/a)^2] \\ F_{mn} &= (1/2) [KA_{55}/\pi^2 + D_{11}(m/a)^2 + D_{66}(n/b)^2] \\ G_{mn} &= (1/2) [KA_{44}/\pi^2 + D_{22}(n/b)^2 + D_{66}(m/a)^2] \\ H_m &= (K/2\pi) A_{55}(m/a) \\ U_n &= (K/2\pi) A_{44}(n/b) \\ Q_{mn} &= (1/2)(D_{12} + D_{66})(m/a)(n/b) \end{aligned} \quad (14)$$

Likewise, the kinetic energy expression [Eq. (2)] becomes

$$T = -\left(\frac{1}{2}\right) \left(\frac{\gamma h}{g}\right) \left(\frac{ab}{4}\right) \sum_m \sum_n \omega^2 a_{mn}^2 \exp(2i\omega t) \quad (15)$$

Introducing Lagrange multipliers, the function to be minimized becomes

$$G = V + T - \sum_{j=1}^q \alpha_j \sum_{m=1}^{\infty} b_{mj} - \sum_{i=1}^p \beta_i \sum_{n=1}^{\infty} d_{in} \quad (16)$$

where α_j ($j = 1, 2, \dots, q$) and β_i ($i = 1, 2, \dots, p$) are the Lagrange multipliers. Substituting Eqs. (13) and (15) into Eq. (16),

$$\begin{aligned} G &= \sum_m \sum_n \left[\bar{E}_{mn} a_{mn}^2 + F_{mn} b_{mn}^2 + G_{mn} d_{mn}^2 + 2H_m a_{mn} b_{mn} + 2U_n a_{mn} d_{mn} + 2Q_{mn} b_{mn} d_{mn} \right. \\ &\quad \left. - \sum_{j=1}^q \alpha_j \sum_{m=1}^{\infty} b_{mj} - \sum_{i=1}^p \beta_i \sum_{n=1}^{\infty} d_{in} \right] \end{aligned} \quad (17)$$

where

$$\bar{E}_{mn} = E_{mn} - (2\gamma h/g)f^2 \quad \text{and} \quad f = \omega/2\pi \quad (18)$$

The minimization equations are

$$\frac{\partial G}{\partial a_{mn}} = \frac{\partial G}{\partial b_{mn}} = \frac{\partial G}{\partial d_{mn}} = 0 \quad (m, n = 1, 2, 3, \dots) \quad (19)$$

Substituting Eq. (17) into these minimization equations and solving these in a matrix form, the following results are obtained:

$$\begin{aligned} a_{mn} &= (2/ab\pi^2) [(U_n Q_{mn} - G_{mn} H_m) \alpha_n \\ &\quad + (H_m Q_{mn} - F_{mn} U_n) \beta_m] / \bar{\Delta}_{mn} \end{aligned} \quad (20)$$

$$\begin{aligned} b_{mn} &= (2/ab\pi^2) [(\bar{E}_{mn} G_{mn} - U_n^2) \alpha_n \\ &\quad + (H_m U_n - \bar{E}_{mn} Q_{mn}) \beta_m] / \bar{\Delta}_{mn} \end{aligned} \quad (21)$$

$$d_{mn} = (2/ab\pi^2) [(H_m U_n - \bar{E}_{mn} Q_{mn}) \alpha_n + (\bar{E}_{mn} F_{mn} - H_m^2) \beta_m] / \bar{\Delta}_{mn} \quad (22)$$

where

$$\bar{\Delta}_{mn} = \bar{E}_{mn} (F_{mn} G_{mn} - Q_{mn}^2) - H_m (H_m G_{mn} - U_n Q_{mn}) + U_n (H_m Q_{mn} - U_n F_{mn}) \quad (23)$$

Substituting Eqs. (21) and (22) into the constraint relationships [Eqs. (11) and (12)], the following equations are ob-

tained:

$$\alpha_j \sum_{m=1}^{\infty} (\bar{E}_{mj} G_{mj} - U_j^2) / \bar{\Delta}_{mj} + \sum_{m=1}^p (H_m U_j - \bar{E}_{mj} Q_{mj}) \beta_m / \bar{\Delta}_{mj} = 0 \quad (j=1, 2, \dots, q) \quad (24)$$

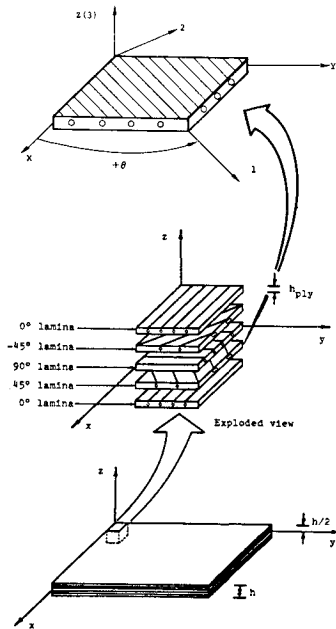


Fig. 1 Laminate geometry and reference coordinates.

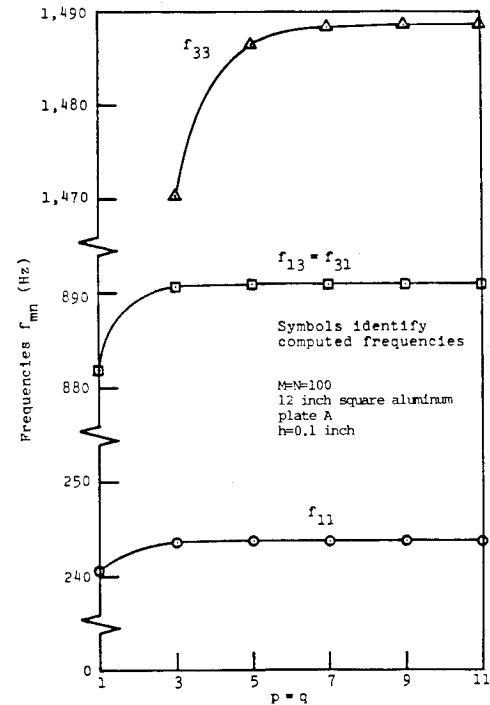


Fig. 2 Effect of p and q on the convergence of natural frequencies of aluminum plate A.

Table 1 Geometry of analyzed plates

| Plate designation | Material | h_{ply} , in. | No. of plies | Layup | h , in. | a , in. | b , in. |
|-------------------|----------------|-----------------|--------------|-------------------------------------|-----------|-----------|-----------|
| A | Aluminum | 0.1000 | 1 | | 0.1000 | 12.0 | 12.0 |
| B | Boron/epoxy | 0.0053 | 8 | $[0]_{8T}$ | 0.0424 | 12.0 | 12.0 |
| C | Boron/epoxy | 0.0053 | 48 | $[0]_{48T}$ | 0.2544 | 12.0 | 12.0 |
| D | Boron/epoxy | 0.0053 | 96 | $[0]_{96T}$ | 0.5088 | 12.0 | 12.0 |
| E | Boron/epoxy | 0.0053 | 144 | $[0]_{144T}$ | 0.7632 | 12.0 | 12.0 |
| F | Boron/epoxy | 0.0053 | 192 | $[0]_{192T}$ | 1.0176 | 12.0 | 12.0 |
| G | Graphite/epoxy | 0.0104 | 48 | $[(\pm 45/0_2)_2/\pm 45/0/90]_{2s}$ | 0.4992 | 25.0 | 9.0 |
| H | Graphite/epoxy | 0.0052 | 48 | $[(\pm 45/0_2)_2/\pm 45/0/90]_{2s}$ | 0.2496 | 25.0 | 9.0 |

Table 2 Properties of analyzed plates

| Property | Laminate designation (see Table 1) | | | |
|--------------------------------|------------------------------------|-----------------------|-----------------------|-----------------------|
| | A | B ^a | G | H |
| D_{11} , lb-in. | 0.93517×10^3 | 0.19827×10^3 | 0.11627×10^6 | 0.14534×10^5 |
| D_{12} , lb-in. | 0.30861×10^3 | 0.48352×10^1 | 0.29929×10^5 | 0.37401×10^4 |
| D_{16} , lb-in. | 0 | 0 | 0.14876×10^4 | 0.18595×10^3 |
| D_{22} , lb-in. | 0.93517×10^3 | 0.17269×10^2 | 0.51323×10^5 | 0.64153×10^4 |
| D_{26} , lb-in. | 0 | 0 | 0.14876×10^4 | 0.18595×10^3 |
| D_{66} , lb-in. | 0.31328×10^3 | 0.47641×10^1 | 0.32259×10^5 | 0.40324×10^4 |
| A_{55} , lb-in. | 0.37594×10^6 | 0.31800×10^5 | 0.39936×10^6 | 0.19968×10^6 |
| A_{44} , lb-in. | 0.37594×10^6 | 0.31800×10^5 | 0.39936×10^6 | 0.19968×10^6 |
| K | 0.82250 | 0.82250 | 0.82250 | 0.82250 |
| γ , lb-in. ³ | 0.10000 | 0.07412 | 0.05753 | 0.05753 |

^a A_{ij} and D_{ij} for laminates C, D, E, and F may be obtained as follows: $A_{ij}(C) = A_{ij}(B) h_C/h_B$, $D_{ij}(C) = D_{ij}(B) h_C^3/h_B^3$, etc., where h_B and h_C are the thicknesses of laminates B and C, respectively (see Table 1).

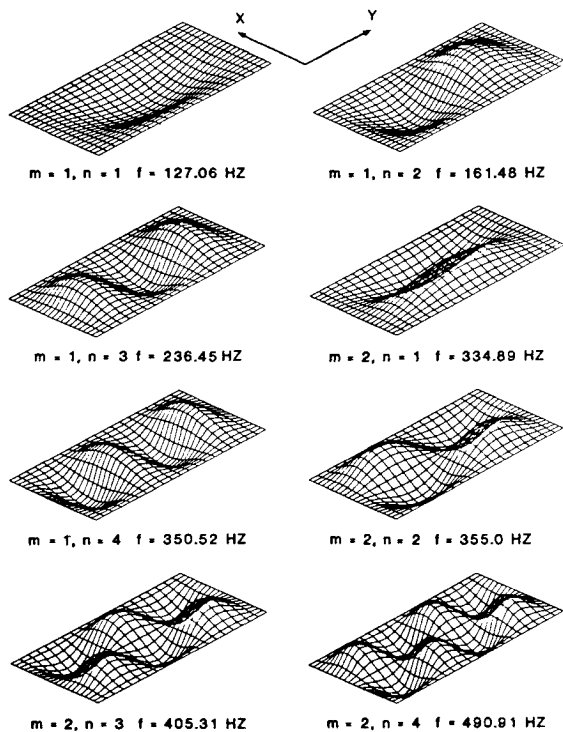


Fig. 3 Natural frequencies and mode shapes for a boron/epoxy laminate (plate B).

$$\sum_{n=1}^q (H_i U_n - \bar{E}_{in} Q_{in}) \alpha_n / \bar{\Delta}_{in} + \beta_i \sum_{n=1}^{\infty} (\bar{E}_{in} F_{in} - H_i^2) / \bar{\Delta}_{in} = 0 \quad (i = 1, 2, \dots, p) \quad (25)$$

These $p + q$ linear homogeneous equations provide a nontrivial solution for the Lagrange multipliers ($\alpha_1, \dots, \alpha_q, \beta_1, \dots, \beta_p$) only when the coefficient matrix is singular (determinant = 0). The frequency values for which this determinant vanishes are referred to as the natural (free vibration) frequencies of the clamped laminate.

The natural frequencies of the clamped laminate are obtained by assuming various frequency values, starting from a value near zero, to determine the values that make the determinant vanish. In conducting this frequency sweep, singularities occur at $\bar{\Delta}_{mn} = 0$. This is because the assumed displacement and slope expressions satisfy all of the boundary conditions for a simply supported orthotropic plate. The singularities, therefore, correspond to the natural frequencies of the simply supported plate.

To avoid the numerical difficulty associated with this, the natural frequencies of the simply supported plate are computed initially⁹ and these values are skipped during the "frequency sweep" operation for the clamped plate. The Lagrange multipliers in Eqs. (24) and (25) represent the point moments that should be applied around the plate boundary to impose zero bending slopes at these locations.

After the natural frequencies of the clamped orthotropic plate are computed using the procedure described above, the corresponding mode shapes are obtained as follows. Each natural frequency is substituted into Eqs. (24) and (25) to obtain the relative values of the α and β . These are subsequently substituted into Eqs. (20-22) to obtain the mode shape corresponding to the selected natural frequency.

The described analytical procedure is an elegant and economical means of obtaining the natural frequencies and the corresponding mode shapes for clamped laminates. Although a finite-element analysis would yield comparable results, a

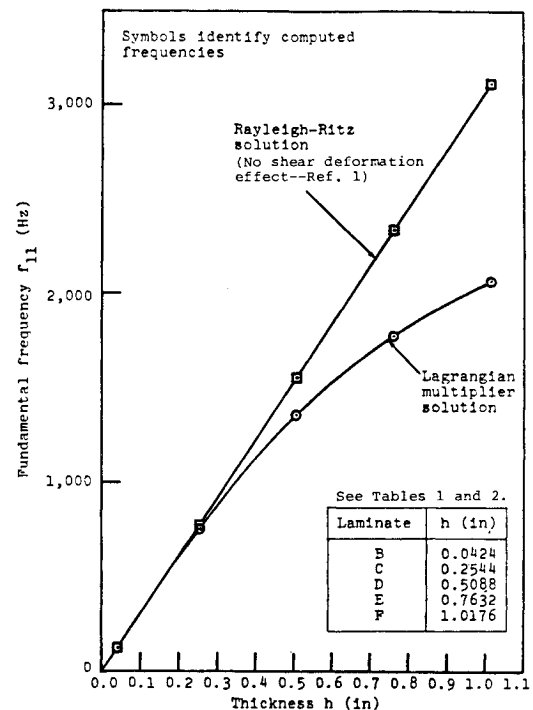


Fig. 4 Effect of shear deformation of f_{11} for unidirectional boron/epoxy laminates.

Table 3 Natural frequencies of an aluminum plate (A)

| m | n | Analytically predicted f_{mn} , Hz | | |
|-----|-----|--------------------------------------|--------|---------------|
| | | Present analysis ^a | Ref. 1 | Difference, % |
| 1 | 1 | 243.8 | 239.7 | 1.68 |
| 1 | 3 | 891.0 | 879.7 | 1.27 |
| 3 | 1 | | | |
| 3 | 3 | 1488.3 | 1467.0 | 1.43 |
| 1 | 5 | 2088.2 | 2058.9 | 1.40 |
| 5 | 1 | | | |
| 3 | 5 | 2652.8 | 2622.7 | 1.13 |
| 5 | 3 | | | |
| 1 | 7 | 3811.7 | 3763.6 | 1.26 |
| 7 | 1 | | | |

^a $p = q = 7$. See Tables 1 and 2 for plate dimensions and properties.

large number of elements would be required to ensure computational accuracy, especially for the higher modes. And, when the results are incorporated into a forced vibration analysis, the finite-element method becomes even more sensitive to the element size around the contact location and is far more expensive than an analytical approach.

Results

The geometry and properties of the analyzed plates are defined in Tables 1 and 2, respectively. The effects of the selected number of Lagrange multipliers (constraint points) and the number of terms in the assumed series for w , ψ_x , and ψ_y as solution convergence are addressed initially. The assumed infinite series [Eqs. (8-10)] yield terms in the coefficient matrix of the eigenvalue problem [Eqs. (24) and (25)] that are summations of infinite terms. In practice, the infinite summations are truncated by assuming finite M and N values to be the maximum values for m and n , respectively. From Eqs. (24) and (25), it is seen that M and N must be greater than or

Table 4 Natural frequencies for a boron/epoxy laminate (plate B)

| <i>m</i> | <i>n</i> | Analytically predicted f_{mn} , Hz | | | Experimentally measured f_{mn} , Hz (Ref. 1) |
|----------|----------|--------------------------------------|--------|---------|--|
| | | Present analysis ^a | Ref. 1 | Ref. 10 | |
| 1 | 1 | 127.06 | 125.0 | 127.55 | 107.0 |
| 1 | 2 | 161.48 | 159.0 | 162.05 | 123.0 |
| 1 | 3 | 236.45 | 232.0 | 236.70 | 204.0 |
| 2 | 1 | 334.89 | 329.0 | 336.01 | 283.0 |
| 1 | 4 | 350.52 | 343.0 | 350.81 | 343.0 |
| 2 | 2 | 355.0 | 350.0 | 357.21 | 301.0 |
| 2 | 3 | 405.31 | 397.0 | 406.01 | 360.0 |
| 2 | 4 | 490.91 | 482.0 | 492.11 | 451.0 |

^a $p = q = 15$; $m, n = 1, 2, \dots, 30$.**Table 5** Analytically predicted natural frequencies for a clamped graphite/epoxy laminate (plate G)

| <i>m</i> | <i>n</i> | f_{mn} , Hz computed using the developed analysis (Lagrangian multiplier method) ^a | | f_{mn} , Hz, computed using the Rayleigh-Ritz solution in Ref. 10 |
|----------|----------|---|--|---|
| | | With shear deformation | Without shear deformation ^b | |
| 1 | 1 | 347.94 | 364.89 | 361.64 |
| 2 | 1 | 425.79 | 454.13 | 449.06 |
| 3 | 1 | 559.25 | 606.85 | 600.69 |
| 4 | 1 | 745.11 | 823.50 | 816.28 |
| 1 | 2 | 881.29 | 960.67 | 951.38 |
| 2 | 2 | 955.03 | 1054.40 | 1044.9 |
| 5 | 1 | 973.37 | 1103.4 | 1094.2 |
| 3 | 2 | 1074.8 | 1209.3 | 1200.6 |
| 4 | 2 | 1240.1 | 1428.5 | 1416.8 |
| 6 | 1 | 1241.3 | 1442.8 | 1432.2 |

^a $p = q = 15$; $m, n = 1, 2, \dots, 30$. ^bActual A_{44} and A_{55} values are multiplied by 1000.

equal to p and q , respectively. In the presented results, M and N were assumed to be $p + q$ each, unless specified otherwise. Figure 2 presents the effect of the number of constraint points (p and q) along each plate edge on the computed natural frequencies. Larger values of p and q are required for the higher modes. But, for the lower modes, a small value of p and q will yield a converged solution. Figure 2 indicates that $p = q = 3$ provides a converged solution for the fundamental mode f_{11} and $p = q = 7$ provides a converged solution for f_{33} .

The first sample problem addresses the natural frequencies of an isotropic plate (plate A in Table 1). The frequencies computed using the developed analysis are compared with predictions based on the Rayleigh-Ritz method.¹ The analysis in Ref. 1 assumes the plate transverse displacement functions to be the known mode shapes for a clamped-clamped beam and does not account for shear deformation effects. Table 3 shows that the frequencies obtained using the developed analysis differ from those predicted by Ref. 1 by less than 2%. The Lagrangian multiplier method, nevertheless, predicts slightly higher frequencies compared to those in Ref. 1.

The second sample problem addresses the natural frequencies of a clamped $[0]_{8T}$ boron/epoxy laminate (plate B in Table 1). Table 4 presents three analytical predictions based on the developed Lagrangian multiplier method and the Rayleigh-Ritz solutions of Refs. 1 and 10. Experimentally measured natural frequencies¹ are also included in Table 4. It is seen that the analytical predictions based on the Lagrangian multiplier method demonstrate an excellent agreement with Rayleigh-Ritz solutions. However, a maximum difference of nearly 20% is noticed between the measured frequencies in Ref. 11 and the analytically predicted values. The mode shapes corresponding to the various natural frequencies, computed by the developed analysis, are displayed in Fig. 3.

Table 6 Analytically predicted natural frequencies for a clamped graphite/epoxy laminate (plate H)

| <i>m</i> | <i>n</i> | f_{mn} , Hz, computed using the developed analysis (Lagrangian multiplier method) ^a | | f_{mn} , Hz, computed using the Rayleigh-Ritz solution in Ref. 10 |
|----------|----------|--|--|---|
| | | With shear deformation | Without shear deformation ^b | |
| 1 | 1 | 179.15 | 182.31 | 181.11 |
| 2 | 1 | 222.66 | 225.68 | 224.89 |
| 3 | 1 | 296.03 | 301.88 | 300.82 |
| 4 | 1 | 399.83 | 410.60 | 408.79 |
| 1 | 2 | 467.81 | 478.79 | 476.45 |
| 2 | 2 | 511.05 | 525.39 | 523.27 |
| 5 | 1 | 531.17 | 550.32 | 547.99 |
| 3 | 2 | 583.26 | 604.62 | 601.28 |
| 4 | 2 | 683.85 | 712.59 | 709.53 |
| 6 | 1 | 688.87 | 720.21 | 717.30 |

^a $p = q = 15$; $m, n = 1, 2, \dots, 30$. ^bActual A_{44} and A_{55} values are multiplied by 1000.

The thickness of the clamped unidirectional boron/epoxy laminate is varied to study the effect of shear deformation on the computed natural frequencies. Retaining the planform dimensions, the number of plies is increased from 8 to 48, 96, 144, and 192 to correspond to laminates C, D, E, and F, respectively, in Tables 1 and 2. Figure 4 presents the effect of plate thickness (shear deformation) on the fundamental frequency of the clamped laminate. The Rayleigh-Ritz solution in Ref. 1 does not account for shear deformation effects and shows the expected linear variation of frequency with thickness. The developed Lagrangian multiplier solution demonstrates a significant shear deformation effect, via a decrease in the frequency with increasing thickness. When the thickness is nearly 1 in., for example, there is a 50% reduction in f_{11} due to shear deformation effects.

Finally, the natural frequencies of 25 in. long, 9 in. wide, AS1/3501/6 graphite/epoxy laminates (plates G and H in Tables 1 and 2) are computed, with and without shear deformation effects. It is noted that the ignored values of D_{16} and D_{26} for these two laminates are small compared to D_{11} , D_{12} , D_{22} , and D_{66} . In the developed Lagrangian multiplier solution, the actual A_{44} and A_{55} terms are multiplied by 1000 to approximate the solution corresponding to infinite transverse shear stiffnesses (no shear deformation). The Rayleigh-Ritz solution in Ref. 10 also does not account for shear deformation effects. Tables 5 and 6 present the analytically predicted natural frequencies for two graphite/epoxy laminates (plates G and H), with and without shear deformation effects. Lagrangian multiplier solutions, assuming large A_{44} and A_{55} values, demonstrate an excellent correlation with Rayleigh-Ritz solutions that do not account for shear deformation effects.¹⁰ As demonstrated earlier, the thicker laminate (plate G) exhibits a larger difference between the shear deformable and nonshear deformable solutions.¹⁰ These differences increase further when higher-order modes are considered.

Conclusions

An analysis was developed, using the Lagrangian multiplier technique, to predict the natural frequencies and mode shapes of clamped isotropic and orthotropic plates. The developed analysis was validated by demonstrating an excellent correlation between its predictions and available Rayleigh-Ritz solutions. These predictions were also in good agreement with available experimental results. The developed analysis was demonstrated to account for the significant shear deformation effects in thick clamped laminates that available Rayleigh-Ritz solutions do not account for. Finally, the validated Lagrangian multiplier solution is currently being incorporated into a dynamic analysis to predict the forced response of clamped orthotropic plates.

Acknowledgment

The work reported here was performed as an Independent Research and Development activity in the Strength and Life Assurance Research Organization at the Northrop Aircraft Division.

References

- ¹Ashton, J.E. and Whitney, J.M., *Theory of Laminated Plates*, Technomic, Stamford, CT, 1970.
- ²Jones, R.M., *Mechanics of Composite Materials*, McGraw-Hill, New York, 1975.
- ³Whitney, J.M. and Pagano, N.J., "Shear Deformation in Heterogeneous Anisotropic Plates," *Transactions of ASME, Journal of Applied Mechanics*, Vol. 92, Dec. 1970, pp. 1031-1036.
- ⁴Mindlin, R.D., "Influence of Rotatory Inertia and Shear on Flexural Motions of Isotropic, Elastic Plates," *Transactions of ASME, Journal of Applied Mechanics*, Vol. 73, March 1951, pp. 31-38.

⁵Budiansky, B., Hu, P.C., and Connor, R.W., "Notes on the Lagrangian Multiplier Method in Elastic-Stability Analysis," NACA TN-1558, 1948.

⁶Dowell, E.H., "Free Vibrations of a Linear Structure with Arbitrary Support Conditions," *Transactions of ASME, Journal of Applied Mechanics*, Vol. 93, Sept. 1971, pp. 595-600.

⁷Sanders, W.J., "Computation of Natural Frequencies of Clamped Laminated Plates Using Lagrangian Multiplier Technique," Master's Thesis, California State University, Long Beach, May 1983.

⁸Reed, D.L., "Laminated Sandwich Panel Analysis," General Dynamics, Convair Aerospace Div., Rept. FZM-5590 prepared for Air Force Materials Laboratory, Oct. 1971.

⁹Dobyns, A.L., "Analysis of Simply-Supported Orthotropic Plates Subject to Static and Dynamic Loads," *AIAA Journal*, Vol. 19, May 1981, pp. 642-650.

¹⁰Northrop-Developed Computer Code based on the structural analysis procedure in Ref. 8.

¹¹Ashton, J.E. and Anderson, J.D., "Natural Modes of Vibration of Boron-Epoxy Plates," *Shock and Vibrations Bulletin*, No. 39, Pt. 4, April 1969.

AIAA Meetings of Interest to Journal Readers*

| Date | Meeting (Issue of <i>AIAA Bulletin</i> in which program will appear) | Location | Call for Papers† |
|-------------|--|---|------------------|
| 1987 | | | |
| March 2-5 | AIAA/SDIO High Power Laser Device Show (Secret) (Jan.) | National Bureau of Standards Boulder, CO | |
| April 6-8 | AIAA/ASME/AHS/ASEE 28th Structures, Structural Dynamics and Materials Conference (Feb.) | Doubletree Hotel Monterey, CA | May 86 |
| June 8-10 | AIAA 19th Fluid Dynamics, Plasma Dynamics and Lasers Conference (April) | Sheraton Waikiki Honolulu, HI | Sept. 86 |
| June 9-11 | AIAA 8th Computational Fluid Dynamics Conference (April) | Sheraton Waikiki Honolulu, HI | Sept. 86 |
| Aug. 17-19 | AIAA 5th Applied Aerodynamics Conference (June) | Doubletree Hotel Monterey, CA | Sept. 86 |
| Oct. 7-9 | AIAA Computers in Aerospace VI (Aug.) | Wakefield, MA | Jan. 87 |

*For a complete listing of AIAA meetings, see the current issue of the *AIAA Bulletin*.

†Issue of *AIAA Bulletin* in which Call for Papers appeared.